研究成果の刊行物・別刷り

Toxicology Letters 212 (2012) 1–10

Contents lists available at SciVerse ScienceDirect

Toxicology Letters

journal homepage: www.elsevier.com/locate/toxlet

Effects of methylmercury exposure on neuronal differentiation of mouse and human embryonic stem cells

Xiaoming He[a,1], Satoshi Imanishi[a,1], Hideko Sone[b,*], Reiko Nagano[b], Xian-Yang Qin[b,c], Jun Yoshinaga[c], Hiromi Akanuma[b], Junko Yamane[a], Wataru Fujibuchi[d], Seiichiroh Ohsako[a]

[a] Division of Environmental Health Sciences, Center for Disease Biology and Integrative Medicine, Graduate School of Medicine, The University of Tokyo, 7-3-1 Hongo, Bunkyo-ku, Tokyo 113-8654, Japan
[b] Research Center for Environmental Risk, National Institute for Environmental Studies, 16-2 Onogawa, Tsukuba, Ibaraki 305-8506, Japan
[c] Department of Environmental Studies, Graduate School of Frontier Science, The University of Tokyo, 5-1-5 Kashiwanoha, Kashiwa, Chiba 270-8563, Japan
[d] Computational Biology Research Center, Advanced Industrial Science and Technology (AIST), 2-4-7 Aomi, Koto-ku, Tokyo 135-0064, Japan

ARTICLE INFO

Article history:
Received 26 January 2012
Received in revised form 13 April 2012
Accepted 16 April 2012
Available online xxx

Keywords:
Methylmercury
Human
Embryonic stem cells
Neuronal development
Alternative method

ABSTRACT

The establishment of more efficient *in vitro* approaches has been widely acknowledged as a critical need for toxicity testing. In this study, we examined the effects of methylmercury (MeHg), which is a well-known developmental neurotoxicant, in two neuronal differentiation systems of mouse and human embryonic stem cells (mESCs and hESCs, respectively). Embryoid bodies were generated from gathering of mESCs and hESCs using a micro-device and seeded onto ornithine–laminin-coated plates to promote proliferation and neuronal differentiation. The cells were exposed to MeHg from the start of neuronal induction until the termination of cultures, and significant reductions of mESCs and hESCs were observed in the cell viability assays at 1,10,100 and 1000 nM, respectively. Although the mESC derivatives were more sensitive than the hESC derivatives to MeHg exposure in terms of cell viability, the morphological evaluation demonstrated that the neurite length and branch points of hESC derivatives were more susceptible to a low concentration of MeHg. Then, the mRNA levels of differentiation markers were examined using quantitative RT-PCR analysis and the interactions between MeHg exposure and gene expression levels were visualized using a network model based on a Bayesian algorithm. The Bayesian network analysis showed that a MeHg-node was located on the highest hierarchy in the hESC derivatives, but not in the mESC derivatives, suggesting that MeHg directly affect differentiation marker genes in hESCs. Taken together, effects of MeHg were observed in our neuronal differentiation systems of mESCs and hESCs using a combination of morphological and molecular markers. Our study provided possible, but limited, evidences that human ESC models might be more sensitive in particular endpoints in response to MeHg exposure than that in mouse ESC models. Further investigations that expand on the findings of the present paper may solve problems that occur when the outcomes from laboratory animals are extrapolated for human risk evaluation.

1. Introduction

Methylmercury (MeHg) has severely poisoned over tens of thousands of individuals in Japan and in Iraq, and exposure to small amounts of MeHg through the consumption of fish, shellfish, or sea mammals continues to be an issue (Airaksinen et al., 2010; Kuntz et al., 2010). Nearly all humans worldwide have trace amounts of MeHg in their tissues, which suggest widespread presence of MeHg in the environment (Grandjean et al., 2010). In addition, MeHg can cause neurotoxicity during pregnancy, even in the absence of maternal toxicity (*i.e.*, the human infants suffered a so-called congenital Minamata disease and exhibit severe developmental disabilities, such as cerebral palsy, mental retardation, convulsive seizures and muscle rigidity) (Davidson et al., 2004; Harada et al., 1999). Despite the simultaneous exposure of a mother and an infant during pregnancy, serious symptoms have not been observed in mothers, which suggests that the fetal brain is highly sensitive to MeHg (Davidson et al., 2004; Harada et al., 1999); however, no information is available on dose–response relationships in

Abbreviations: MeHg, methylmercury; DMSO, dimethyl sulfoxide; MSA, microsphere-array; EB, embryoid body; hESC, human embryonic stem cell; mESC, mouse embryonic stem cell; EST, embryonic stem cell test; hNPC, human neuronal precursor cells; ECVAM, European Center for the Validation of Alternative Methods; ICA, IN Cell Analyzer.

* Corresponding author. Tel.: +81 29 850 2464; fax: +81 29 850 2546.
E-mail address: hsone@nies.go.jp (H. Sone).

[1] These authors contributed equally.

0378-4274/$ – see front matter © 2012 Elsevier Ireland Ltd. All rights reserved.
http://dx.doi.org/10.1016/j.toxlet.2012.04.011

these children. Laboratory mice and rats do not exhibit the typical symptoms of congenital Minamata disease following similar MeHg exposures during pregnancy despite frequent fetal and infant deaths following exposure to a relatively low dose of MeHg *in utero* (Choi, 1989; Hu et al., 2010; Satoh and Suzuki, 1983; Weiss et al., 2005). These findings suggest that the susceptibility of developing neuronal cells in the human fetus to MeHg is distinct and more severe from the susceptibility of laboratory animals.

Embryonic stem cells (ESCs) can differentiate *in vitro* into cells of all three embryonic germ layers, which reflect to some extent, the *in vivo* development of the embryo. This concept has provided the scientific rationale for emerging research on the use of ESCs to establish tests for toxicity to the early embryo. An embryonic stem cell test (EST) using a cardiac differentiation system from mouse ESCs (mESCs) is advocated by the European Center for the Validation of Alternative Methods (ECVAM) as one of alternative methods for *in vivo* embryo toxicity (Genschow et al., 2004). Researchers believe that the development of an EST that is based on human ESCs (hESCs) will provide an ideal tool for the assessment of human embryo toxicity because such a system will improve the prediction of human hazards while reducing the requirement for laboratory animals. In addition, a hESC-based EST would limit the need to consider interspecies differences (Reubinoff et al., 2000; Thomson et al., 1998). Many researchers are currently attempting to develop a human EST to evaluate the effects of chemicals on cardiac and neuronal differentiation (Murabe et al., 2007; Stummann and Bremer, 2008; Stummann et al., 2009; Wada et al., 2009).

The toxicity of MeHg has been examined in several ESCs-derived neural developmental models and the endpoints generally used included cell survival, cell morphology, transcript changes, and so on (Baek et al., 2011; Stummann et al., 2009; Tamm et al., 2006; Theunissen et al., 2011). In this study, we described two neuronal differentiation systems of mESCs and hESCs and examined the effects of MeHg using a combination of morphological and molecular markers. The advantages of our study might include: (1) the use of mouse *vs.* human ESCs provided a potential approach to explore/understand species differences; (2) the incorporation of the morphological endpoint in addition to the usual mRNA expression could provide detailed mechanistic insight to improve the EST for the assessments of developmental neurotoxicants.

2. Materials and methods

2.1. Culture and neuronal differentiation of ESCs

The mESC line, B6G-2 (XY genotype), was provided from RIKEN BioResource Center and maintained as described (Shimizukawa et al., 2005). The hESC line, KhES-3 (XY genotype), was provided by Dr. Hirofumi Suemori, Research Center of Stem Cells, Institute for Frontier Medical Science, Kyoto University (Suemori et al., 2006). All experiments using hESCs were approved by the ethics committees of the National Institute for Environmental Studies and the University of Tokyo in accordance with to the guideline of the Japanese Ministry of Education, Culture, Sports, Science, and Technology. The procedures for the maintenance of mESCs and hESCs were performed as described previously (Shimizukawa et al., 2005; Suemori et al., 2006). Both mESCs and hESCs were allowed to form embryoid bodies (EBs) in the micro-device of microsphere-array (MSA; 1020 holes, φ 300 μm/hole, STEM Biomethods, Japan). The EBs were seeded onto ornithine–laminin (O/L)-coated 24-well plates to promote proliferation and neuronal differentiation with the sequential exchange of authentic appropriate neuronal differentiation media. The schedules for the neuronal differentiation of mESCs and hESCs are summarized in Figs. 1A and 2B, respectively. Exposure to MeHg (0.001% DMSO) began on Day 12 or Day 27 and continued until Day 23 or Day 50 for the mESC and hESC derivatives, respectively. The medium containing MeHg was refreshed every 3 days (see details in Supplemental Material, Methods).

2.2. MTT assay

Cytotoxicity was measured in terms of reduced mitochondrial activity using the MTT-Assay Kit. EB-derived cells were plated onto O/L-coated 96-well plates, and a 10-μl aliquot of 3-(4,5-dimethyl-2-thiazolyl)-2,5-diphenyltetrazolium bromide was added to the cells at each time point and incubated for 4 h. After incubation, 100-μl of isopropyl alcohol was added. Following additional 24-h incubation, the optical density was measured at 570 nm. Standard curves were prepared for each cell type by counting cells derived from mESCs and hESCs that were cultured in medium without MeHg or DMSO.

2.3. Immunocytochemistry

Immunostaining of MAP2 was performed on Day 23 for mESCs (mESC-Day 23) and Day 50 for hESCs (hESC-Day 50). After fixation for 10 min with 4% paraformaldehyde, the cells were permeabilized in 0.1% Triton X-100 in PBS. The cells were incubated with 1% BSA, which was followed by overnight incubation with primary antibody specific for MAP2 (1:200). After PBS washing, the cells were incubated at room temperature for 1 h with Alexa 568-labeled secondary antibodies (1:1000). Nuclei were stained using 2 μg/ml of Hoechst 33342 for 15 min.

2.4. Morphological measurement by IN Cell Analyzer

Microphotographs were periodically obtained using Olympus IX70 22FL/PH inverted microscope (Olympus Optical, Japan). The morphological analysis was performed using an automatic multichannel imaging analyzer (IN Cell Analyzer 1000 (ICA), GE Healthcare UK Ltd., Buckinghamshire, UK). The microphotographs of 57 fields (0.60 mm^2) per well of 24 well plate (*i.e.*, 1368 fields per exposure group) were taken automatically. The fields in a well were created without overlap. The fluorescent signal detected by the 535-nm laser line combined with a HQ620 60 M emission filter was considered to be the MAP2-positive signal of neurons. The fluorescent signal detected using the 360-nm laser line combined with a HQ460 40 M emission filter was considered to indicate the Hoechst33342 positive nuclei. Fluorescence emission was separately recorded in the blue and red channels, and a flat field correction was applied for inhomogeneous illumination of the scanned area for each of the two channels.

A typical merged image of hESC-derivatives is shown in Fig. S1A. Hoechst-positive nuclei were recognized using IN Cell Developer Software (GE Healthcare UK Ltd.) and replaced by yellow dots to accurately count the nuclei number (Fig. S1B). MAP2-positive signals were also recognized by this software with a threshold appropriate for tracing the MAP2-postive neurites. The replaced pink images are shown in Fig. S1C. MAP2-positive signals surrounding nuclei were regarded as the cell bodies of differentiated neural cells. The number of nuclei within the cell body was considered to be the number of MAP2-positive neurons in each field. The areas considered to be cell bodies were subtracted from the MAP2-postive images to generate the image of the neurites as shown in Fig. S1D. Then the software automatically replaces the MAP2-positive neurite images with branching morphologies, which indicated neurite-length as green center lines and branching points as blue circles (Figs. S1D, S1E, and S1F). As shown in Supplemental Fig. S1E, the cell bodies were successfully distinguished from the neurites. The total length of the MAP2-positive projection was automatically measured on its midline (Fig. S1F). The values for neurite length/cell were calculated by dividing the total MAP2-positive neurite length within a field by the number of MAP2-positive neurons. The branching points of MAP2-positive projections were automatically counted as the total number of branching points of the MAP2-positive projections (Fig. S1F). The values for branching points/cell were calculated by dividing the total MAP2-positive neurite branching points within a field by the number of MAP2-positive neurons. The average of the neurite length/cell or branching points/cell of all fields in one well of the 24-well plate were indicated as the value of one experiment. Images of mESC-derived neuronal cells were analyzed in the same manner.

To evaluate the accuracy of ICA measurements, the total neurite lengths of 5 randomly selected fields were manually measured using ImageJ (IJ) software (NIH). The correlations between data from IN Cell Developer Software and from IJ are shown in Fig. S2. Although the values obtained by ICA tended to be higher (approximately 1.73-fold for neurite length and 4.42-fold for branching points), the two values obtained by ICA and IJ were well correlated, which demonstrated the accuracy of the ICA measurement.

2.5. Quantitative RT-PCR

Total RNA from the mESC or hESC derivatives was harvested with an RNeasy mini kit. Gene expression of neuronal differentiation markers (Table 1) in the mESC and hESC derivatives were investigated by semi-quantitative RT-PCR or quantitative RT-PCR (see primer information in Supplemental Material, Table S1) using a high-throughput real-time thermal cycler (Light Cycler 480 system, Roche, Basel, Switzerland). The quantitative data were obtained by calculating the absolute copy number as previously described (Sakata et al., 2007).

2.6. Network model analysis

The linkages between MeHg and differentiation marker gene indices were visualized using a network model that was based on a Bayesian algorithm modified from an algorithm defined in a previous study (Toyoshiba et al., 2004). In brief, the network was quantified to calculate the posterior probability distribution for the strength of the linkages on the basis of the gene expression datasets (see Supplemental Material, Table S2 and Table S3). A network was used to evaluate

the ability of the algorithm to have a higher posterior probability (p-value) at the correct linkage in the network (see the detail described in Supplemental Material, Methods).

2.7. Statistical analysis

Statistical analyses were performed with StatView for Windows, version 5.0 (SAS Institute, Cary, NC). All data were expressed relative to the means of the control groups. All results are represented as mean ± SE. A two-way analysis of variance (ANOVA) was used for the MTT assay to compare the effect of each dose with the DMSO control groups. Other data were analyzed by one-way ANOVA followed by Fisher's PLSD post hoc test. p-Values less than 0.05 were considered to be statistically significant.

Table 1
Selection of neuronal differentiation markers in this study.

Gene	Function	Reference
NODAL	Mesoendoderm formation	Tada et al. (2005)
PAX6	Cerebral cortex formation	Caric et al. (1997), Duparc et al. (2006)
EMX2	Cerebral cortex formation	Galli et al. (2002), Mallamaci et al. (2000)
Hoxb4	Paraximal mesoderm formation	Brend et al. (2003)

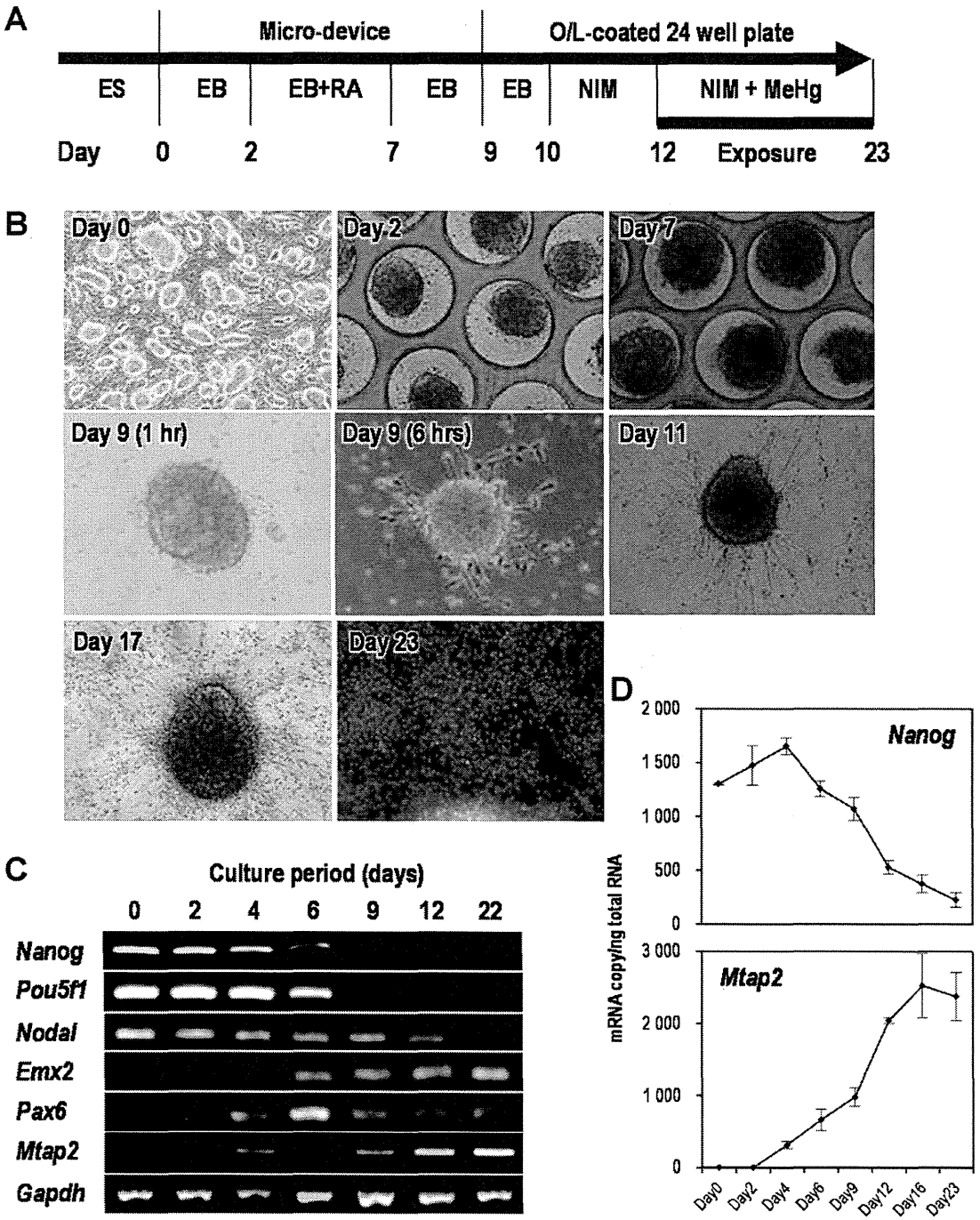

Fig. 1. Neuronal differentiation culture systems form mouse and human ESCs. (A and E) Schemesfor culture conditions and MeHg exposure using mESCs and hESCs (see details in Supplemental Materials, Methods). (B and F) Typical features of mESC and hESC colonies, mouse and human EBs growing in the micro-device, and differentiating neuronal cells. The values in parentheses are time after plating. Day 23 in mESCs and Day 50 in hESCs show MAP2 immunostaining, respectively. (C and G) Semi-quantitative RT-PCR analysis for differentiation marker genes. (D and H) Quantitative RT-PCR analysis for *Nanog*/*NANOG* and *Map2*/*MAP2* mRNAs. *Mtap2*/*MTAP2* is a official symbol of *Map2*/*MAP2*.

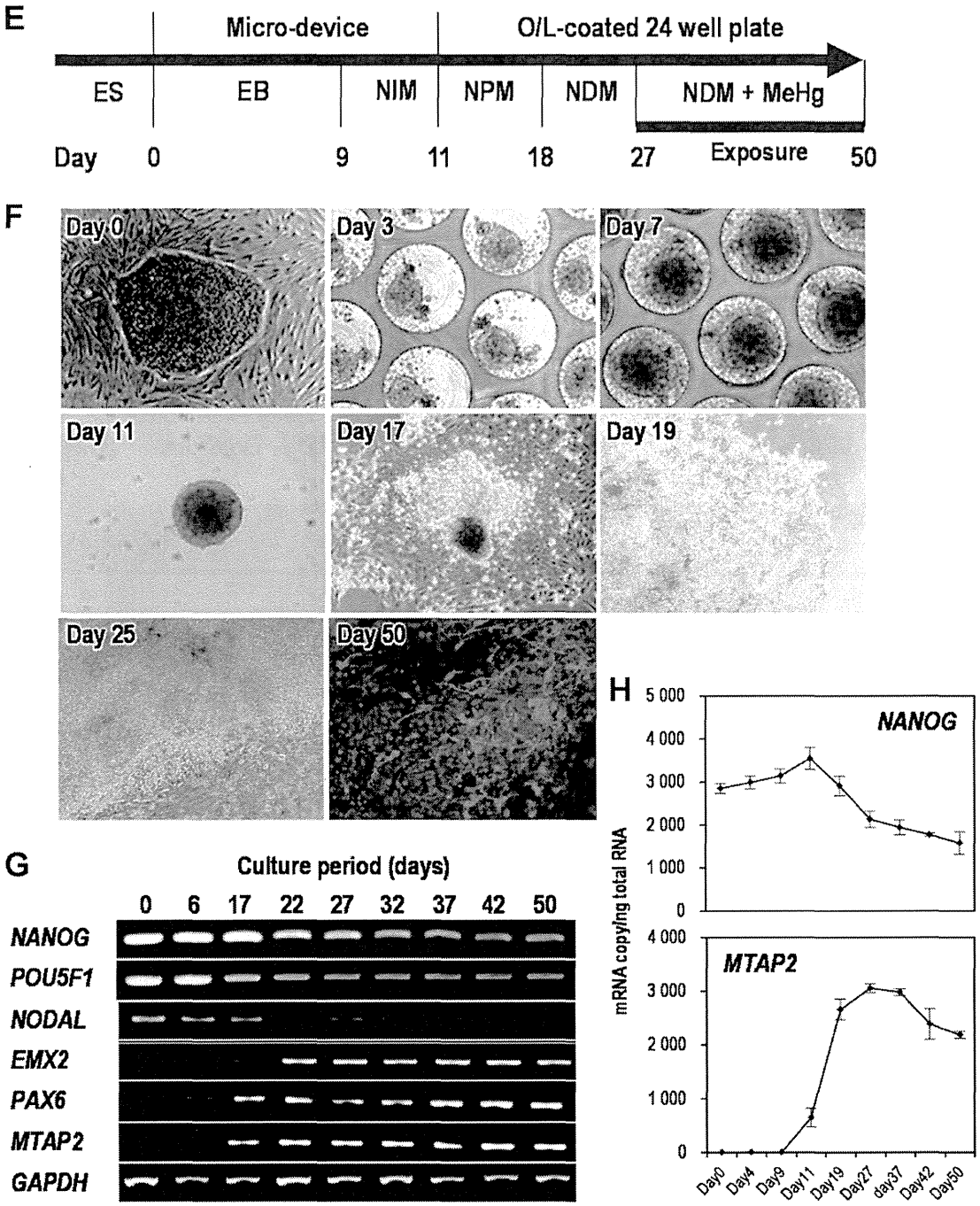

Fig. 1. (*Continued*).

3. Results

3.1. Neuronal differentiation of mESC and hESC derivatives

Typical features of neuronal differentiation from mESCs and hESCs are represented in Fig. 1B and F, respectively. In the mESC culture, EBs were generated in MSA and attached to O/L-coated dishes on Day 9. The migrating neuron-like cells appeared by Day 17. The *Nanog* mRNA level was decreased around Day 6 and became 17.3% at the end of culture (Fig. 1D). The neuronal lineage makers *Emx2*, *Pax6*, and *Map2* mRNAs were first detected on Day 4 and became stronger throughout neuronal induction (Fig. 1C). In contrast, the hESC derivatives continued to grow colonially and neuron-like cells appeared by Day 50 (Fig. 1F). In addition, *EMX2*, *PAX6*, and *MAP2* mRNAs were first detected around hESC-Day 17 (Fig. 1G), which was later compared with the mESC cultures (Fig. 1C). Although the *NANOG* mRNA was decreased around on Day 22, approximately one-half of the mRNAs were maintained till Day 50 (Fig. 1H).

3.2. Effects of MeHg on mESC and hESC derivatives cell viability

Based on the mRNA expression levels of neuronal differentiation markers, we considered that the mESC-Day 12 and the hESC-Day 27 cultures were similar stages of early neuronal development. MeHg exposure began on mESC-Day 12 and hESC-Day 27 and we measured the relative MTT activities compared with control (DMSO) for each time point (Fig. 2). The mESC-derived cells had completely disappeared within 5 days after the 1000 nM MeHg exposure (Fig. 2A),

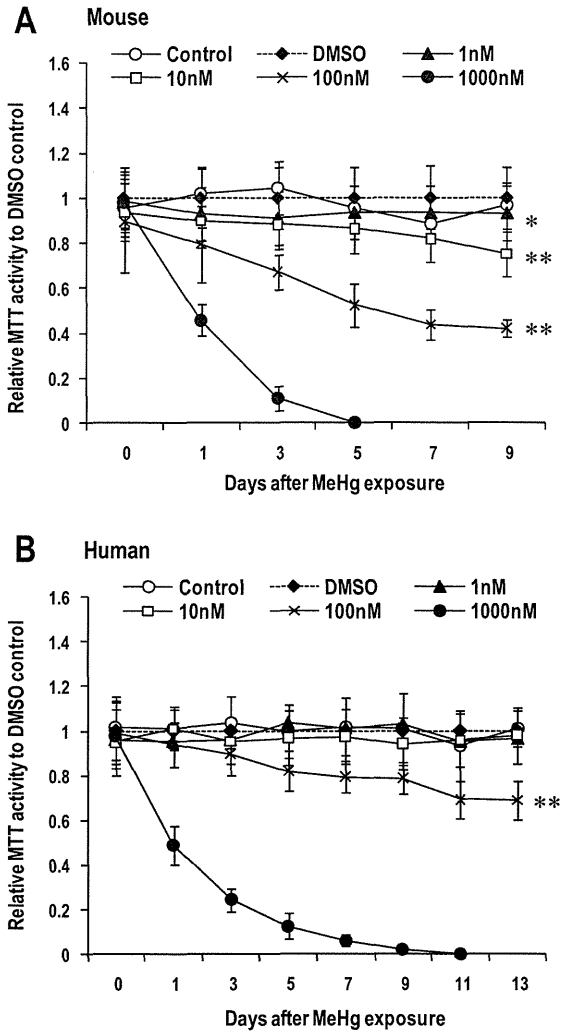

Fig. 2. Cytotoxicity of MeHg exposure to mESC- (A) and hESC-derived (B) neuronal cells. Serially diluted concentrations of MeHg were applied to the cells for the MTT assay (1, 10, 100 and 1000 nM). Cell viabilities for the DMSO control at each time point were used for normalization. Two-way ANOVA was used to determine the statistical difference ($^{*}p < 0.05$; $^{**}p < 0.01$).

whereas, it took 11 days for the same effect to be observed in the hESC derivatives (Fig. 2B). Significant decreases in mESCs cell viability were observed at 9 days after 1, 10 and 100 nM MeHg exposure. In contrast, we only observed a significant reduction in MTT activity in hESCs at 13 days after 100 nM MeHg exposure.

3.3. Effects of MeHg on morphologies of mESC and hESC derivatives

Typical MAP2-immunostainings at the end of the cell culturing period are shown in Fig. 3A and B. In mESC derivatives, the nuclear count was significantly decreased in the 100 nM group (0.16-fold) (Fig. 3C), and this result occurred from the drastic decrease in the viability of mESC derived cells (Fig. 2A). Conversely, significant differences in nuclear count were not found in the hESC derivatives (Fig. 3C). The Map2-positive neurite density from mESC derivatives was significantly decreased at the highest dose of MeHg (0.17-fold at 100 nM), whereas that of the hESCs was significantly decreased in all MeHg exposed groups (0.26-fold at 1 nM, 0.04-fold at 10 nM and 0.05-fold at 100 nM) (Fig. 3D). Furthermore, analysis of Map2-positive neurite lengths and branching points using ICA revealed that MeHg induced changes in morphological properties (Fig. 3E and F). With more details, significant reduce in Map2-positive neurite lengths was observed only at 100 nM group in mESC-derivatives (0.48-fold), while there was a significant dose-dependent decrease in neurite length in the hESCs, even at the lowest dose (Fig. 3E). The number of branching points in both mESC- and hESC-derivatives was only significantly reduced at 100 nM MeHg (0.54-fold and 0.65-fold, respectively) (Fig. 3F).

3.4. Effects of MeHg on the differentiation markers of mESC and hESC derivatives

Quantitative RT-PCR was performed at the end of the cell culturing period to investigate the effect of MeHg on the mRNA levels of the differentiation markers, especially those involved in central nervous system development. Although the mRNA copy numbers for the undifferentiated marker gene *Nanog* (mESC) and *NANOG* (hESC) were quite different from each other in control groups, they were increased by MeHg exposure (Fig. 4A and B). However, no significant increase in *Nanog* expression was observed in mESC-derivatives, while significant increases in *NANOG* expression were observed in 10 nM and 100 nM group in hESC-derivatives. For both mESC and hESC-derivatives, the TGFβ-family gene *NODAL* showed a definite tendency to be increased in a dose-dependent manner (Fig. 4A and B). However, significant increase was observed only in 100 nM group in hESC-derivatives. The neruroectoderm marker gene *PAX6* was significantly decreased by MeHg treatment in human cells in 10 nM and 100 nM groups (Fig. 4B). The mRNA levels of *EMX2* were also significantly deceased at the three doses in hESC-derivatives (Fig. 4B). The levels of the dendrite marker *MAP2* in both mESC and hESC-derivatives were significantly decreased at 100 nM MeHg. The expression of *Hoxb4* was significantly decreased in mESC-derivatives at 100 nM MeHg. Conversely, *HOXB4* showed significant dose-dependent upregulation in hESCs with the increasing concentrations of MeHg (Fig. 4B).

3.5. Network models

The interaction between MeHg exposure and gene expression levels observed in the PCR analyses was converted into network models using a Bayesian algorithm. In accordance with the principle of the previous reports (Friedman et al., 2000; Imoto et al., 2002), the regulatory effects of increasing amounts of chemical on mRNA levels can be evaluated in terms of a probabilistic inference. For mESC-derivatives, when p-value was defined over 0.5, the MeHg node dominated only five genes: *En1*, *Nodal*, *Nes*, *Otx1*, and *Hoxb1* (Fig. 5A). In hESC-derivatives, the MeHg node was located at the top of a network hierarchy and was related directly or indirectly to all the evaluated genes (Fig. 5B).

4. Discussion

The present study attempted to investigate the effects of MeHg in mESC- and hESC-derived neural developmental models using a combination of morphological and molecular markers. Numerous EBs of similar sizes were generated from both mESCs and hESCs using a unique micro-device (Sakai et al., 2010). With the exceptions of media, which was optimized for each culture, and differences in the MeHg exposure period, we attempted to adjust each protocol to be as similar to each other as possible. The concentrations of MeHg used to treat mESC and hESC in our study were 1,10,100 and 1000 nM, respectively. These concentrations are almost the same as levels detected in human whole blood (Grandjean et al., 1998).

The neuronal differentiation of hESCs generally requires a longer period than that of mESCs, which is likely due to the species-specific program. Watanabe and colleagues reported similar protocols for

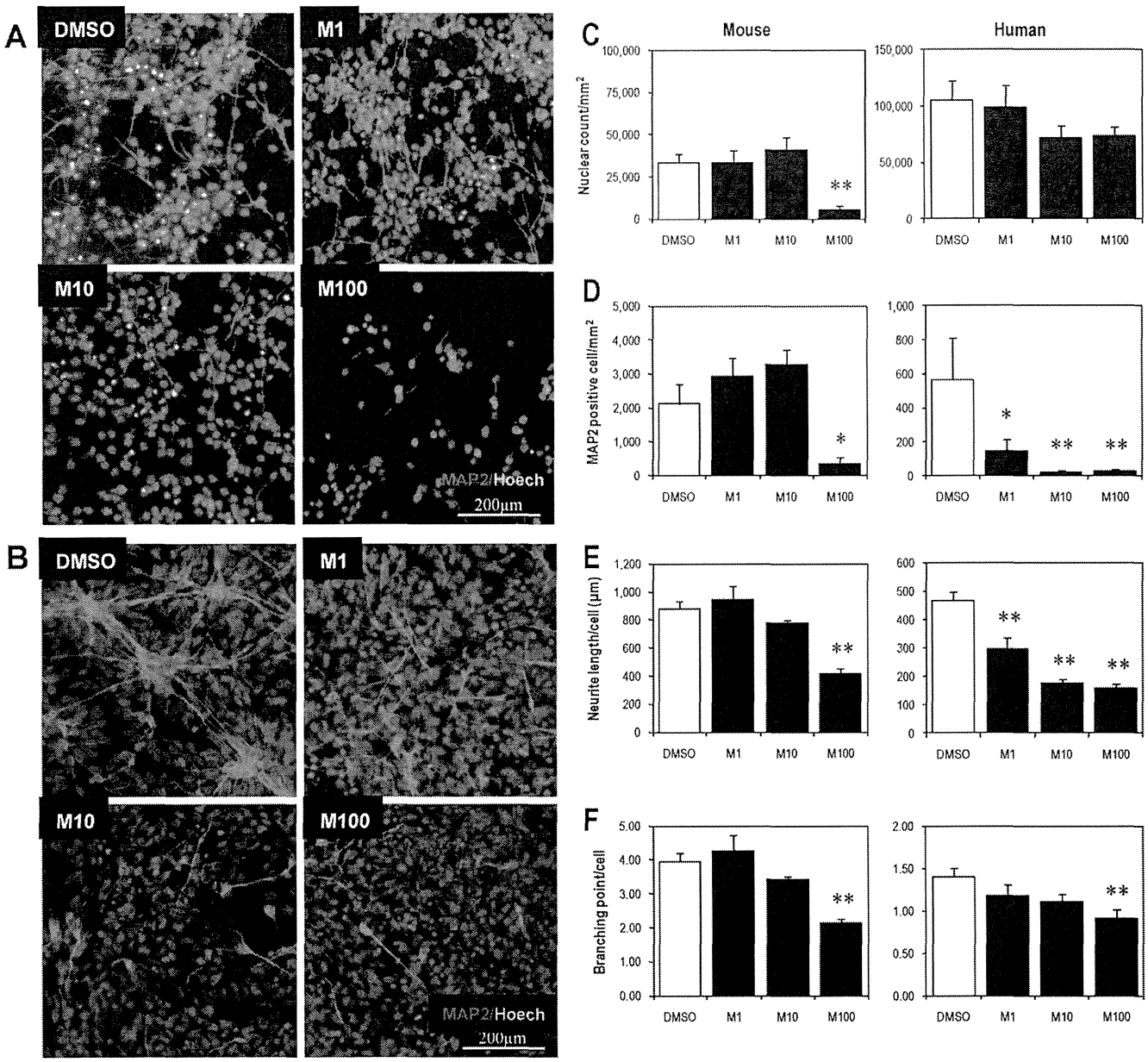

Fig. 3. The effect of MeHg exposure on the mESC- and hESC-derived neuronal cells. (A) Microphotographs of mESC neuronal derivatives on Day 23 (B) and hESC neural derivatives on Day 50. DMSO, control group; M1, 1 nM MeHg; M10, 10 nM of MeHg; M100, 100 nM of MeHg. Red: MAP2, blue: nucleus stained with Hoechst 33342. (C–F) Morphological measurement by high throughput automatic imaging analyzer (ICA) (see details in Supplemental Materials, Methods and Figs. S1 and S2). Data from 24-well culture plates were expressed as mean ± SE ($n = 6$). (C) Nuclear count per area. (D) MAP2-positive cell number per area. (E) Neurite length per cell. (F) Branching points per cell. One-way ANOVA followed by Fisher's PLSD test as post hoc were used to determine the statistical difference from DMSO control (*$p < 0.05$; **$p < 0.01$). (For interpretation of the references to color in this figure legend, the reader is referred to the web version of the article.)

the neuronal differentiation of mESCs and hESCs based on EB formation in serum-free suspension cultures (Eiraku et al., 2008; Watanabe et al., 2005, 2007). According to their reports, telencephalic precursors appeared within 5 days in the case of mESCs, whereas it took 35 days in the case of hESCs. Consistent with their reports, our study initially detected the expression of the neuronal marker genes on Day 4 in mESCs and on Day 17 in hESCs (Fig. 1C and G). At the end of culture, the mRNA copy numbers of *Map2* (mouse) on Day 23 and *MAP2* (human) on Day 50 were approximately equal, suggesting that the similar amounts of mature neural derivatives were successfully differentiated from both ESCs (Fig. 1D and H). In the morphological analysis, neuron proliferation was observed until Day 17 for mESC-derivatives, whereas the hESC-derivatives proliferated colonially in attached cultures on Day 42, and neuron proliferation was observed until Day 50 (Fig. 1B and 1E). These observations agree with previous studies that have examined the neuronal differentiation of both mESCs and hESCs (Nat et al., 2007; Song et al., 2008; Wada et al., 2009). Then, we exposed the cells to MeHg starting on Day 12 for mESCs and Day 27 for hESC because these times allowed for equivalent stages of development in both cell lines.

In utero exposure to MeHg causes severe neurodegenerative effects in human fetuses, which is known as congenital Minamata disease in Japan (Harada, 1978). In Iraq, neurodegenerative effects of MeHg have been attributed to the accidental ingestion of MeHg-contaminated wheat (Bakir et al., 1973). Whether human susceptibility to MeHg is greater than that of laboratory animals is not clear. According to the results of numerous *in vitro* studies using neuronal cell-lines of rodents and human, there is a tendency for human cells to be more susceptible to MeHg

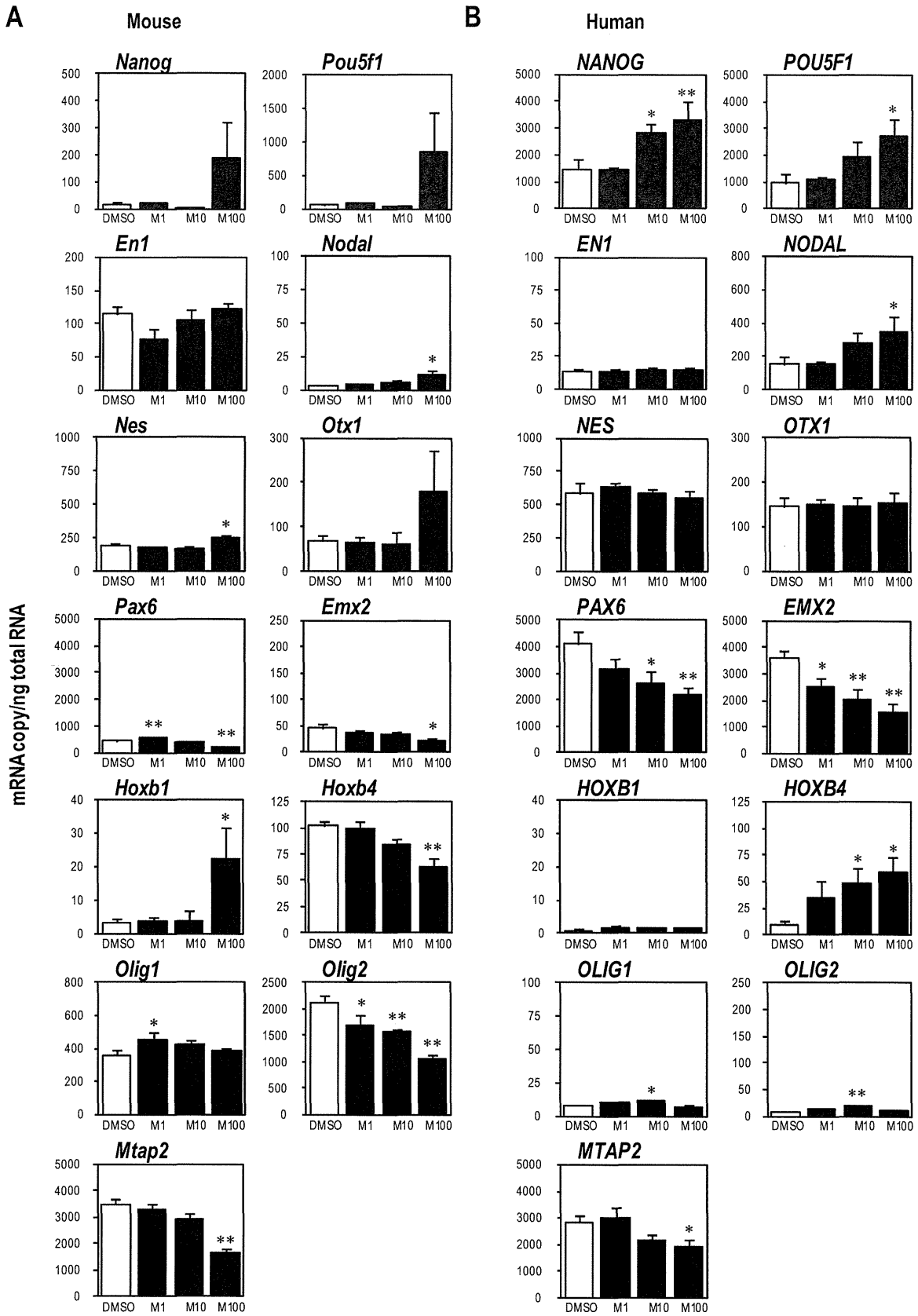

Fig. 4. The effect of MeHg exposure on the gene expression in mESC (A) and hESC (B) derivatives at the end of culture. Expression levels were calculated as absolute copy numbers of target mRNAs per total RNA. Data from 24-well culture plates were expressed as mean ± SE ($n = 6$). DMSO, control group; M1, 1 nM of MeHg; M10, 10 nM of MeHg; M100, 100 nM of MeHg. One-way ANOVA followed by Fisher's PLSD test as post hoc were used to determine the statistical difference from DMSO control (*$p < 0.05$; **$p < 0.01$).

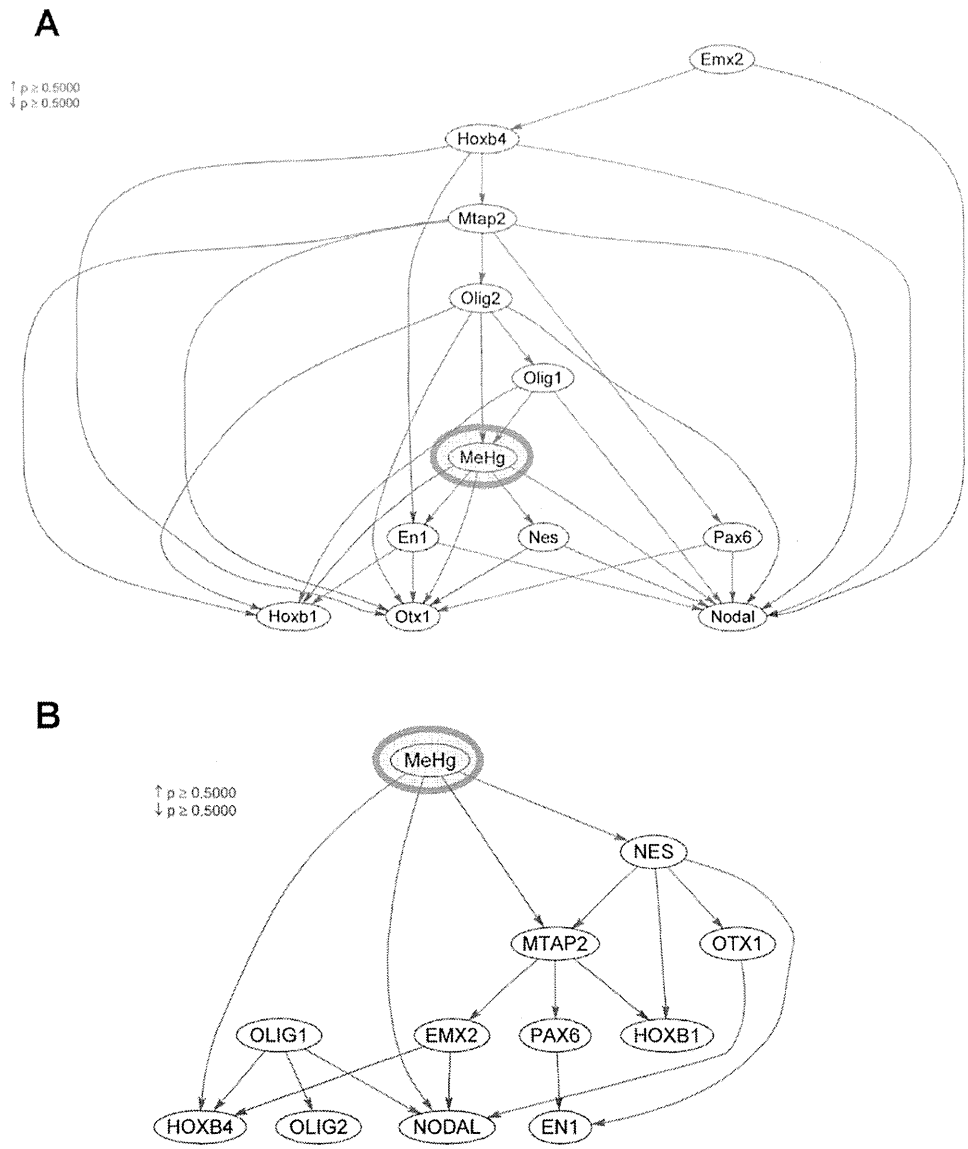

Fig. 5. Bayesian network models for the effect of MeHg exposure on the mESC (A) and hESC (B) derivatives. Correlations among chemical concentrations (MeHg: red circle) and gene expression levels (11 genes) were analyzed and drawn automatically by a computer software. The β-value of the Bayesian model was expressed as a red arrow if positively relative, and a blue arrow if negatively relative. The correlation probability ($p > 0.05$) was defined in the analysis. (For interpretation of the references to color in this figure legend, the reader is referred to the web version of the article.)

poisoning (Ceccatelli and Moors, 2010). Some of the behavioral effects of MeHg in rodents remain controversial, and the methods for modeling human MeHg exposure in animals require further optimization (Liang et al., 2009). For example, in a murine prenatal exposure model, MeHg (31.9 nmol/g food) accumulated at approximately 25 μg/g fetal brain and resulted in approximately 40% total embryonic/fetal death (Satoh and Suzuki, 1983). Interestingly, other than subtle defects in working memory, visual spatial ability, and anxiety-like behavior, no neurological defects were detected following the accumulation of 12.8–13.3 μg/g brain of mice (Liang et al., 2009). In human epidemiological studies, the highest level of MeHg in umbilical cords from the patients with congenital Minamata disease was 1.60 ± 1.00 ppm (Harada et al., 1999). Although it is difficult to comment on interspecies differences using previous published studies, taken together, they suggest that human susceptibility to MeHg is greater than that of mice, particularly with regard to the functional status of developing neurons. In this present study, our cytotoxicity assays and morphological analyses provided possible, but limited, evidences that cell death in immature mouse neuronal cells occurs at lower doses of MeHg than that in humans, although the morphology and functional status of the surviving cells remain normal. In contrast, the abnormal differentiation and maturation of neurons in humans may begin at lower concentrations of MeHg than those required for cell death, which could result in neuro-performance symptoms in infants. However, it should be noted that the density of Map2-positive cells was different between our mESC and hESC models, which might also affect their sensitivities to MeHg exposure.

In our study, the reductions in gene expression levels for *PAX6* and *EMX2* were clearly detected in hESC-derivatives exposed to low doses of MeHg. On the other hand, the deletion or mutation of *Pax6* or *Emx2* in mice has been reported to cause severe cortical dysplasia in mouse (Caric et al., 1997; Mallamaci et al., 2000). Furthermore, a human genetic study showed that the *PAX6* gene had a dosage effect in a family with congenital cataracts, aniridia, anophthalmia and central nervous system defects (Glaser et al., 1994). These suggest that both *PAX6* and *EMX2* genes may cooperate in the proliferation and differentiation of neuronal stem cells

and the migration of neuronal progenitors during the formation of the cerebral cortex in the fetus.

Bayesian network analysis has been reported to predict gene interaction networks and protein-protein interactions (Friedman et al., 2000; Imoto et al., 2002; Jansen et al., 2003; Pe'er et al., 2001). The Bayesian network is drawn as a directed acyclic graph, having a direction with a hierarchy in which a parent node affects the child node(s). Therefore elements that exert more effects should be located higher in the hierarchy of a calculated network model. In the toxicological studies, Bayesian network analysis has been used to map the dose-dependent response of biomarkers to chemical exposures (Hack et al., 2010; Nagano et al., 2012; Yang et al., 2010). According to our analysis of mESC-derived cells, the node for MeHg was located to the middle of hierarchy, which suggested that MeHg toxicity could not be more definitively mapped because of the slight effects at lower doses. In contrast, the node for MeHg in hESCs was located to the top of network hierarchy, which suggested that MeHg affects the differentiation of neuronal cells in hESCs more significantly than it does in the mESCs, although differences between these two culture systems, such as the time frame of the neuronal differentiation process, length of exposure, and composition of the culture media, should also be taken into consideration (Fig. 5B).

The EST endorsed by ECVAM includes a cytotoxicity assay and a cardiac differentiation inhibition assay using mESC cells. Twenty test chemicals with known *in vivo* embryo toxic potential, including MeHg, were tested in blind conditions, and good reproducibility was achieved (*i.e.*, an accuracy of 78%) (Genschow et al., 2004). MeHg exposure studies in a mESC neuronal differentiation system found an IC_{50} value of 260 nM using resazurin cytotoxicity test of 14 days continuous exposure (Stummann et al., 2007). Consistent with our study, there was a decrease in *Map2* mRNA expression at 100 nM, which was a non-cytotoxic concentration (Stummann et al., 2007). The hESC neuronal differentiation system has been also used to test the embryo toxic potential of MeHg by the same research team (Stummann et al., 2009). Following 12 days continuous exposure (cytotoxicity, IC_{50} value = 39 nM), the neuronal marker genes *NEUROD1* and *MAP2* showed significant decreases of 55% and 29%, respectively, in the presence of 25 nM MeHg. Although the cytotoxicity data for mESCs were different from the present data, the data from hESCs were similar. In addition to significant reductions in the expression of *PAX6* and *EMX2* at MeHg exposure levels less than 10 nM, there was a tendency for a reduction of *MAP2* expression, which suggested a consistent dose-response for human neuronal development.

Human neuronal precursor cells (hNPC) can be used as an alternative model to test human susceptibility to developmental neurotoxicants (Moors et al., 2009). An hNPC can differentiate into neurons in approximately one week, which is an advantage over human ESTs. Based on the ratio of hNPC derived Tuj1-positive neuron and migration activity, more than 500 nM of MeHg showed toxic effect (Moors et al., 2009), which suggests a much higher level of resistance than that observed in the present study. This large difference may be due to the different differentiation states of hNPCs at the time of MeHg exposure compared with those of human neuronal progenitors from ESCs. Indeed, the progenitors produced in our culture system (Day 27) may have been more immature, which could have increased their sensitivity to MeHg. Despite continuous exposure for an extended time (23 days), the present results showed that differentiated MAP2-positive neuronal cells were able to survive (Fig. 3B). This observation indicated that mature neuronal cells are more resistant to MeHg than immature cells. Therefore, ESTs appear to evaluate embryo toxicity more effectively than an hNPC culture system. For example, the critical window for observing psychiatric defects (*e.g.*, autism spectrum disorder) as a result of thalidomide exposure is suspected to occur before 25 days of postfertilization (Miller et al., 2005). The effects of chemicals such as thalidomide on earlier stages can only be analyzed with ESTs, which clearly highlights the advantages of human ESTs over hNPCs.

In summary, we examined the effects of MeHg in a low concentration range of 1–1000 nM on the neural differentiation of mESCs and hESCs using a battery of tests, including cell viability assay, morphological and molecular assessments, and network analysis. Our study provided possible, but limited, evidences that human ESC models might be more sensitive in particular endpoints in response to MeHg exposure than that in mouse ESC models. Further investigations that expand on the findings of the present paper may solve problems that occur when the outcomes from laboratory animals are extrapolated for human risk evaluation.

Conflict of interest statement

The authors declare that they have no competing financial interests.

Acknowledgments

This study was supported in part by the Environmental Technology Development Fund (to H. S.) from the Ministry of the Environment and the Grant in Aid for Scientific Research from the Ministry of the Health and Labor (to S. O.), Japan. The authors gratefully acknowledge the technical support of Miss Noriko Oshima (GE Healthcare Japan Corporation) in the analysis using IN Cell Analyzer 1000 and Dr Shigeru Koikegami (Second Lab, LLC) in constructing software for a Bayesian algorithm. The authors also thank Miss Masami Yokoyama for her technical assistance.

Appendix A. Supplementary data

Supplementary data associated with this article can be found, in the online version, at http://dx.doi.org/10.1016/j.toxlet.2012.04.011.

References

Airaksinen, R., Turunen, A.W., Rantakokko, P., Mannisto, S., Vartiainen, T., Verkasalo, P.K., 2010. Blood concentration of methylmercury in relation to food consumption. Public Health Nutrition 14, 480–489.

Baek, D.H., Kim, T.G., Lim, H.K., Kang, J.W., Seong, S.K., Choi, S.E., Lim, S.Y., Park, S.H., Nam, B.H., Kim, E.H., Kim, M.S., Park, K.L., 2011. Embryotoxicity assessment of developmental neurotoxicants using a neuronal endpoint in the embryonic stem cell test. Journal of Applied Toxicology, http://dx.doi.org/10.1002/jat. 1747.

Bakir, F., Damluji, S.F., Amin-Zaki, L., Murtadha, M., Khalidi, A., al-Rawi, N.Y., Tikriti, S., Dahahir, H.I., Clarkson, T.W., Smith, J.C., Doherty, R.A., 1973. Methylmercury poisoning in Iraq. Science 181, 230–241.

Brend, T., Gilthorpe, J., Summerbell, D., Rigby, P.W., 2003. Multiple levels of transcriptional and post-transcriptional regulation are required to define the domain of Hoxb4 expression. Development 130, 2717–2728.

Caric, D., Gooday, D., Hill, R.E., McConnell, S.K., Price, D.J., 1997. Determination of the migratory capacity of embryonic cortical cells lacking the transcription factor Pax-6. Development 124, 5087–5096.

Ceccatelli, S., Daré, E., Moors, M., 2010. Methylmercury-induced neurotoxicity and apoptosis. Chemico-Biological Interactions 188, 301–308.

Choi, B.H., 1989. The effects of methylmercury on the developing brain. Progress in Neurobiology 32, 447–470.

Davidson, P.W., Myers, G.J., Weiss, B., 2004. Mercury exposure and child development outcomes. Pediatrics 113, 1023–1029.

Duparc, R.H., Boutemmine, D., Champagne, M.P., Tetreault, N., Bernier, G., 2006. Pax6 is required for delta-catenin/neurojugin expression during retinal, cerebellar and cortical development in mice. Developmental Biology 300, 647–655.

Eiraku, M., Watanabe, K., Matsuo-Takasaki, M., Kawada, M., Yonemura, S., Matsumura, M., Wataya, T., Nishiyama, A., Muguruma, K., Sasai, Y., 2008. Self-organized formation of polarized cortical tissues from ESCs and its active manipulation by extrinsic signals. Cell Stem Cell 3, 519–532.

Friedman, N., Linial, M., Nachman, I., Pe'er, D., 2000. Using Bayesian networks to analyze expression data. Journal of Computational Biology 7, 601–620.

Galli, R., Fiocco, R., De Filippis, L., Muzio, L., Gritti, A., Mercurio, S., Broccoli, V., Pellegrini, M., Mallamaci, A., Vescovi, A.L., 2002. Emx2 regulates the proliferation of stem cells of the adult mammalian central nervous system. Development 129, 1633–1644.

Genschow, E., Spielmann, H., Scholz, G., Pohl, I., Seiler, A., Clemann, N., Bremer, S., Becker, K., 2004. Validation of the embryonic stem cell test in the international ECVAM validation study on three in vitro embryotoxicity tests. Alternatives to Laboratory Animal 32, 209–244.

Glaser, T., Jepeal, L., Edwards, J.G., Young, S.R., Favor, J., Maas, R.L., 1994. PAX6 gene dosage effect in a family with congenital cataracts, aniridia, anophthalmia and central nervous system defects. Nature Genetics 7, 463–471.

Grandjean, P., Weihe, P., White, R.F., Debes, F., 1998. Cognitive performance of children prenatally exposed to safe levels of methylmercury. Environmental Research 77 (May (2)), 165–172.

Grandjean, P., Satoh, H., Murata, K., Eto, K., 2010. Adverse effects of methylmercury: environmental health research implications. Environmental Health Perspectives 118, 1137–1145.

Hack, C.E., Haber, L., Maier, A., Shulte, P., Fowler, B., Lotz, W.G., Savage Jr., R.E., 2010. A Bayesian network model for biomarker-based dose response. Risk Analysis 30, 1037–1051.

Harada, M., 1978. Congenital Minamata disease: intrauterine methylmercury poisoning. Teratology 18, 285–288.

Harada, M., Akagi, H., Tsuda, T., Kizaki, T., Ohno, H., 1999. Methylmercury level in umbilical cords from patients with congenital Minamata disease. Science of the Total Environment 234, 59–62.

Hu, G.Q., Jin, M.H., Lin, X.L., Guo, C.X., Zhang, L., Sun, Z.W., 2010. Mercury distribution in neonatal rat brain after intrauterine methylmercury exposure. Environmental Toxicology and Pharmacology 29, 7–11.

Imoto, S., Goto, T., Miyano, S., 2002. Estimation of genetic networks and functional structures between genes by using Bayesian networks and nonparametric regression. Pacific Symposium on Biocomputing 7, 175–186.

Jansen, R., Yu, H., Greenbaum, D., Kluger, Y., Krogan, N.J., Chung, S., Emili, A., Snyder, M., Greenblatt, J.F., Gerstein, M., 2003. A Bayesian networks approach for predicting protein-protein interactions from genomic data. Science 302, 449–453.

Kuntz, S.W., Ricco, J.A., Hill, W.G., Anderko, L., 2010. Communicating methylmercury risks and fish consumption benefits to vulnerable childbearing populations. Journal of Obstetric, Gynecologic, and Neonatal Nursing 39, 118–126.

Liang, J., Inskip, M., Newhook, D., Messier, C., 2009. Neurobehavioral effect of chronic and bolus doses of methylmercury following prenatal exposure in C57BL/6 weanling mice. Neurotoxicology and Teratology 31, 372–381.

Mallamaci, A., Mercurio, S., Muzio, L., Cecchi, C., Pardini, C.L., Gruss, P., Boncinelli, E., 2000. The lack of Emx2 causes impairment of Reelin signaling and defects of neuronal migration in the developing cerebral cortex. Journal of Neuroscience 20, 1109–1118.

Miller, M.T., Stromland, K., Ventura, L., Johansson, M., Bandim, J.M., Gillberg, C., 2005. Autism associated with conditions characterized by developmental errors in early embryogenesis: a mini review. International Journal of Developmental Neuroscience: the Official Journal of the International Society for Developmental Neuroscience 23, 201–219.

Moors, M., Rockel, T., Abel, J., Cline, J.E., Gassmann, K., Schreiber, T., Schuwald, J., Weinmann, N., Fritsche, E., 2009. Human neurospheres as three-dimensional cellular systems for developmental neurotoxicity testing. Environmental Health Perspectives 117, 1131–1138.

Murabe, M., Yamauchi, J., Fujiwara, Y., Hiroyama, M., Sanbe, A., Tanoue, A., 2007. A novel embryotoxic estimation method of VPA using ES cells differentiation system. Biochemical and Biophysical Research Communications 352, 164–169.

Nagano, R., Akanuma, H., Qin, X.Y., Imanishi, S., Toyoshiba, H., Yoshinaga, J., Ohsako, S., Sone, H., 2012. Multi-parametric profiling network based on gene expression and phenotype data: a novel approach to developmental neurotoxicity testing. International Journal of Molecular Sciences 13, 187–207.

Nat, R., Nilbratt, M., Narkilahti, S., Winblad, B., Hovatta, O., Nordberg, A., 2007. Neurogenic neuroepithelial and radial glial cells generated from six human embryonic stem cell lines in serum-free suspension and adherent cultures. Glia 55, 385–399.

Pe'er, D., Regev, A., Elidan, G., Friedman, N., 2001. Inferring subnetworks from perturbed expression profiles. Bioinformatics 17 (Suppl. 1), S215–S224.

Reubinoff, B.E., Pera, M.F., Fong, C.Y., Trounson, A., Bongso, A., 2000. Embryonic stem cell lines from human blastocysts: somatic differentiation in vitro. Nature Biotechnology 18, 399–404.

Sakai, Y., Yoshida, S., Yoshiura, Y., Mori, R., Tamura, T., Yahiro, K., Mori, H., Kanemura, Y., Yamasaki, M., Nakazawa, K., 2010. Effect of microwell chip structure on cell microsphere production of various animal cells. Journal of Bioscience and Bioengineering 110, 223–229.

Sakata, Y., Yoshioka, W., Tohyama, C., Ohsako, S., 2007. Internal genomic sequence of human CYP1A1 gene is involved in superinduction of dioxin-induced CYP1A1 transcription by cycloheximide. Biochemical and Biophysical Research Communications 355, 687–692.

Satoh, H., Suzuki, T., 1983. Embryonic and fetal death after in utero methylmercury exposure and resultant organ mercury concentrations in mice. Industrial Health 21, 19–24.

Shimizukawa, R., Sakata, A., Hirose, M., Takahashi, A., Iseki, H., Liu, Y., Kunita, S., Sugiyama, F., Yagami, K., 2005. Establishment of a new embryonic stem cell line derived from C57BL/6 mouse expressing EGFP ubiquitously. Genesis 42, 47–52.

Song, T., Chen, G., Wang, Y., Mao, G., Bai, H., 2008. Chemically defined sequential culture media for TH+ cell derivation from human embryonic stem cells. Molecular Human Reproduction 14, 619–625.

Stummann, T.C., Bremer, S., 2008. The possible impact of human embryonic stem cells on safety pharmacological and toxicological assessments in drug discovery and drug development. Current Stem Cell Research & Therapy 3, 118–131.

Stummann, T.C., Hareng, L., Bremer, S., 2007. Embryotoxicity hazard assessment of methylmercury and chromium using embryonic stem cells. Toxicology 242, 130–143.

Stummann, T.C., Hareng, L., Bremer, S., 2009. Hazard assessment of methylmercury toxicity to neuronal induction in embryogenesis using human embryonic stem cells. Toxicology 257, 117–126.

Suemori, H., Yasuchika, K., Hasegawa, K., Fujioka, T., Tsuneyoshi, N., Nakatsuji, N., 2006. Efficient establishment of human embryonic stem cell lines and long-term maintenance with stable karyotype by enzymatic bulk passage. Biochemical and Biophysical Research Communications 345, 926–932.

Tada, S., Era, T., Furusawa, C., Sakurai, H., Nishikawa, S., Kinoshita, M., Nakao, K., Chiba, T., 2005. Characterization of mesoendoderm: a diverging point of the definitive endoderm and mesoderm in embryonic stem cell differentiation culture. Development 132, 4363–4374.

Tamm, C., Duckworth, J., Hermanson, O., Ceccatelli, S., 2006. High susceptibility of neural stem cells to methylmercury toxicity: effects on cell survival and neuronal differentiation. Journal of Neurochemistry 97, 69–78.

Theunissen, P.T., Pennings, J.L., Robinson, J.F., Claessen, S.M., Kleinjans, J.C., Piersma, A.H., 2011. Time-response evaluation by transcriptomics of methylmercury effects on neural differentiation of murine embryonic stem cells. Toxicological Sciences 122, 437–447.

Thomson, J.A., Itskovitz-Eldor, J., Shapiro, S.S., Waknitz, M.A., Swiergiel, J.J., Marshall, V.S., Jones, J.M., 1998. Embryonic stem cell lines derived from human blastocysts. Science 282, 1145–1147.

Toyoshiba, H., Yamanaka, T., Sone, H., Parham, F.M., Walker, N.J., Martinez, J., Portier, C.J., 2004. Gene interaction network suggests dioxin induces a significant linkage between aryl hydrocarbon receptor and retinoic acid receptor beta. Environmental Health Perspectives 112, 1217–1224.

Wada, T., Honda, M., Minami, I., Tooi, N., Amagai, Y., Nakatsuji, N., Aiba, K., 2009. Highly efficient differentiation and enrichment of spinal motor neurons derived from human and monkey embryonic stem cells. PLoS One 4, e6722.

Watanabe, K., Kamiya, D., Nishiyama, A., Katayama, T., Nozaki, S., Kawasaki, H., Watanabe, Y., Mizuseki, K., Sasai, Y., 2005. Directed differentiation of telencephalic precursors from embryonic stem cells. Nature Neuroscience 8, 288–296.

Watanabe, K., Ueno, M., Kamiya, D., Nishiyama, A., Matsumura, M., Wataya, T., Takahashi, J.B., Nishikawa, S., Nishikawa, S., Muguruma, K., Sasai, Y., 2007. A ROCK inhibitor permits survival of dissociated human embryonic stem cells. Nature Biotechnology 25, 681–686.

Weiss, B., Stern, S., Cox, C., Balys, M., 2005. Perinatal and lifetime exposure to methylmercury in the mouse: behavioral effects. Neurotoxicology 26, 675–690.

Yang, X., Zhang, B., Molony, C., Chudin, E., Hao, K., Zhu, J., Gaedigk, A., Suver, C., Zhong, H., Leeder, J.S., Guengerich, F.P., Strom, S.C., Schuetz, E., Rushmore, T.H., Ulrich, R.G., Slatter, J.G., Schadt, E.E., Kasarskis, A., Lum, P.Y., 2010. Systematic genetic and genomic analysis of cytochrome P450 enzyme activities in human liver. Genome Research 20, 1020–1036.

Int. J. Mol. Sci. **2012**, *13*, 187-207; doi:10.3390/ijms13010187

OPEN ACCESS

International Journal of
Molecular Sciences
ISSN 1422-0067
www.mdpi.com/journal/ijms

Article

Multi-Parametric Profiling Network Based on Gene Expression and Phenotype Data: A Novel Approach to Developmental Neurotoxicity Testing

Reiko Nagano [1,†], Hiromi Akanuma [1,†], Xian-Yang Qin [1,2,†], Satoshi Imanishi [3], Hiroyoshi Toyoshiba [1], Jun Yoshinaga [2], Seiichiroh Ohsako [3] and Hideko Sone [1,*]

[1] Health Risk Research Section, Research Center for Environmental Risk, National Institute for Environmental Studies, 16-2 Onogawa, Tsukuba 305-8506, Japan; E-Mails: nagano.reiko@tasc-nt.or.jp (R.N.); akanuma.hiromi@nies.go.jp (H.A.); y_qin@envhlth.k.u-tokyo.ac.jp (X.-Y.Q.); Toyoshiba_Hiroyoshi@takeda.co.jp (H.T.)

[2] Department of Environmental Studies, Graduate School of Frontier Science, The University of Tokyo, 5-1-5 Kashiwanoha, Kashiwa, Chiba 270-8563, Japan; E-Mail: junyosh@k.u-tokyo.ac.jp

[3] Center for Disease Biology and Integrative Medicine, The University of Tokyo, 7-3-1 Hongo, Bunkyo-ku, Tokyo 113-8654, Japan; E-Mails: imanishi@m.u-tokyo.ac.jp (S.I.); ohsako@m.u-tokyo.ac.jp (S.O.)

† These authors contributed equally to this work.

* Author to whom correspondence should be addressed; E-Mail: hsone@nies.go.jp; Tel.: +81-29-850-2464; Fax: +81-29-850-2546.

Received: 3 October 2011; in revised form: 14 November 2011 / Accepted: 30 November 2011 / Published: 23 December 2011

Abstract: The establishment of more efficient approaches for developmental neurotoxicity testing (DNT) has been an emerging issue for children's environmental health. Here we describe a systematic approach for DNT using the neuronal differentiation of mouse embryonic stem cells (mESCs) as a model of fetal programming. During embryoid body (EB) formation, mESCs were exposed to 12 chemicals for 24 h and then global gene expression profiling was performed using whole genome microarray analysis. Gene expression signatures for seven kinds of gene sets related to neuronal development and neuronal diseases were selected for further analysis. At the later stages of neuronal cell

differentiation from EBs, neuronal phenotypic parameters were determined using a high-content image analyzer. Bayesian network analysis was then performed based on global gene expression and neuronal phenotypic data to generate comprehensive networks with a linkage between early events and later effects. Furthermore, the probability distribution values for the strength of the linkage between parameters in each network was calculated and then used in principal component analysis. The characterization of chemicals according to their neurotoxic potential reveals that the multi-parametric analysis based on phenotype and gene expression profiling during neuronal differentiation of mESCs can provide a useful tool to monitor fetal programming and to predict developmentally neurotoxic compounds.

Keywords: developmental neurotoxicity; embryonic stem cells; high-content screening; Bayesian network modeling; gene expression; multi-parametric analysis

1. Introduction

One of the emerging issues in developmental neurotoxicology is to detect effects of chemicals on fetal programming, which is defined as variations in metabolism, gene expression and genome modification during fetal life that induce or repress the somatic structure and physiological systems after development [1–4]. A significant issue in the prevention of neurodevelopmental deficits of chemical origin is the paucity of testing of chemicals for developmental neurotoxicity [5]. New, precautionary approaches that recognize the unique vulnerability of the developing brain are needed for testing and to control the use of chemicals.

Toxicity testing using embryonic stem cells (ESCs) is an efficient approach for developmental neurotoxicity testing (DNT) [6,7]. Compared with the DNT in animal studies, which are costly, time-consuming, and require considerable numbers of laboratory animals, the ESCs test is unique in that, in a relatively simple cell-line-based assay, it incorporates the entire differentiation route from pluripotent ESCs into differentiated cells [8]. Furthermore, as the neuronal differentiation of ESCs provides insight into the early neurogenesis during embryonic development, several protocols have been developed based on the disturbances of this process to model developmental neurotoxicity [9,10]. A 13-day neural differentiation protocol of mouse embryonic stem cells (mESCs), which is combined with morphological observation, immunocytochemistry, gene expression and flow cytometry, has been applied to assess the developmental neurotoxicity of methyl mercury chloride [9]. More recently, a broad gene expression profile during a 20-day differentiation process of mESCs has been successfully designed, in which transcription-based end points have been used to identify the disturbed neuronal differentiation of mESCs [10]. Developing neurons display plasticity in the type of neurotransmitter phenotype that they can assume, and alterations of synaptic activity and expression of neurotrophic factors can influence the "wiring" of developing neuronal circuits [11]. Consequently, exposure to environmental chemicals that promote or interfere with synaptic activity or expression/function of neurotrophins can result in miswiring, leading to neurobehavioral anomalies. However, a sensitive

method for quantitatively measuring alterations of fetal programming during neuronal differentiation, particularly in the connection between the early disturbances and the later outcomes, has not yet been devised.

Here, we produced a high-content and sensitive method for quantitatively measuring the developmental neuronal toxicity of 12 environmental chemicals (see Table 1) using mESCs test combined with DNA microarray analysis, morphological analysis and Bayesian approaches. This confers a new predictive insight for chemical screening in a complex cell culture system that mimics early mammalian embryonic development. We performed multi-parametric profiling of gene expression data sampled at the early stage of mESC differentiation and neuronal phenotype data sampled at a later stage of neuronal cell differentiation after embryoid body (EB) formation. Then, these sampled data were analyzed by a Bayesian network analysis (BNA). This analysis can be depicted graphically to represent the probability structure of the causal complex [12–14].

Table 1. Summary of 12 test chemicals.

Chemical Name	Ellipsis	Intended Use	Physiological Effect and Toxicity	Mode of Action	Target Protein
Triiodotyronine	T3	Endogenenous hormne	Pseudo thyroid hormone	transcriptional regulation	Thyroid hormone receptor (TR)α, TRβ
Dexamethazone	DEX	Medicinal drug	Pseudo corticosteroid hormone	transcriptional regulation	Glucocorticoid receptor (GR)
17b-Estradiol	E2	Endogenenous hormne		transcriptional regulation	Estrogen receptor (ER)α, ERβ
5a-Dihydrotestosterone	DHT	Endogenenous hormne		transcriptional regulation	Androgen receptor (AR)
2,3,7,8-tetrachlorodibenzo-*p*-dioxin	TCDD	Unintentional chemical	Multi-toxicity	transcriptional regulation	Aryl hydrocarbon receptor (AhR)
Methoprene acid	MPA	Pesticides	Teretogenecity	transcriptional regulation	Retinoid X receptor (RXR)α, RXRβ, RXRγ
Cyclopamine	CPM	Medicinal drug	Teretogenecity	Signal inhibition	Hadgehog signaling pathway
Thalidmide	TMD	Medicinal drug	Teretogenecity and Autism	Unknown	Oxidative stress
4(OH)-2′,3,3′,4′,5′-pentachlorobephenyl 107	PCB	Metabolite of PBC	Multi-toxicity	Unknown	Unknown (ERα, oxidativestress)
Permethrin	PMT	Pesticides	Neuro-toxicity	Unknown	Oxidative stress
Bisphenol A	BPA	Plastic materials	Reproductive and Neuro-toxicity?	Unknown	Unknown (ERα, ERRγ)
Bis(2-ethylhexyl) phthalate	DEHP	Plastic materials	Reproductive and Neuro-toxicity?	Unknown	Unknown [Peroxisome proliferator-activated receptor (PPAR)α, antiTR]

The Bayesian algorithm used in this study was proposed by Toyoshiba *et al.* as a prediction tool for the effect of exposure to chemicals [15]. The TAO-Gen algorithm is based on the assumption of a linear relationship between changes in the expression levels of two genes following chemical exposure [16], which employs the Gibbs sampling method on the search algorithm to estimate posterior probability distribution [17,18]. The advantage of Gibbs sampling is that it samples from a full conditional distribution and it is an efficient and easy sampling procedure. Gibbs sampling is a Markov chain Monte Carlo method, which involves generating a sample from one or several variables with an acceptance probability of one. This process is repeated until the sampled probability distribution is close to the actual distribution. This algorithm can be used to search for key transcription factors of signal transduction during ES cell differentiate process [19].

Figure 1. Experimental steps in this study for the assessment of developmental neurotoxicity.

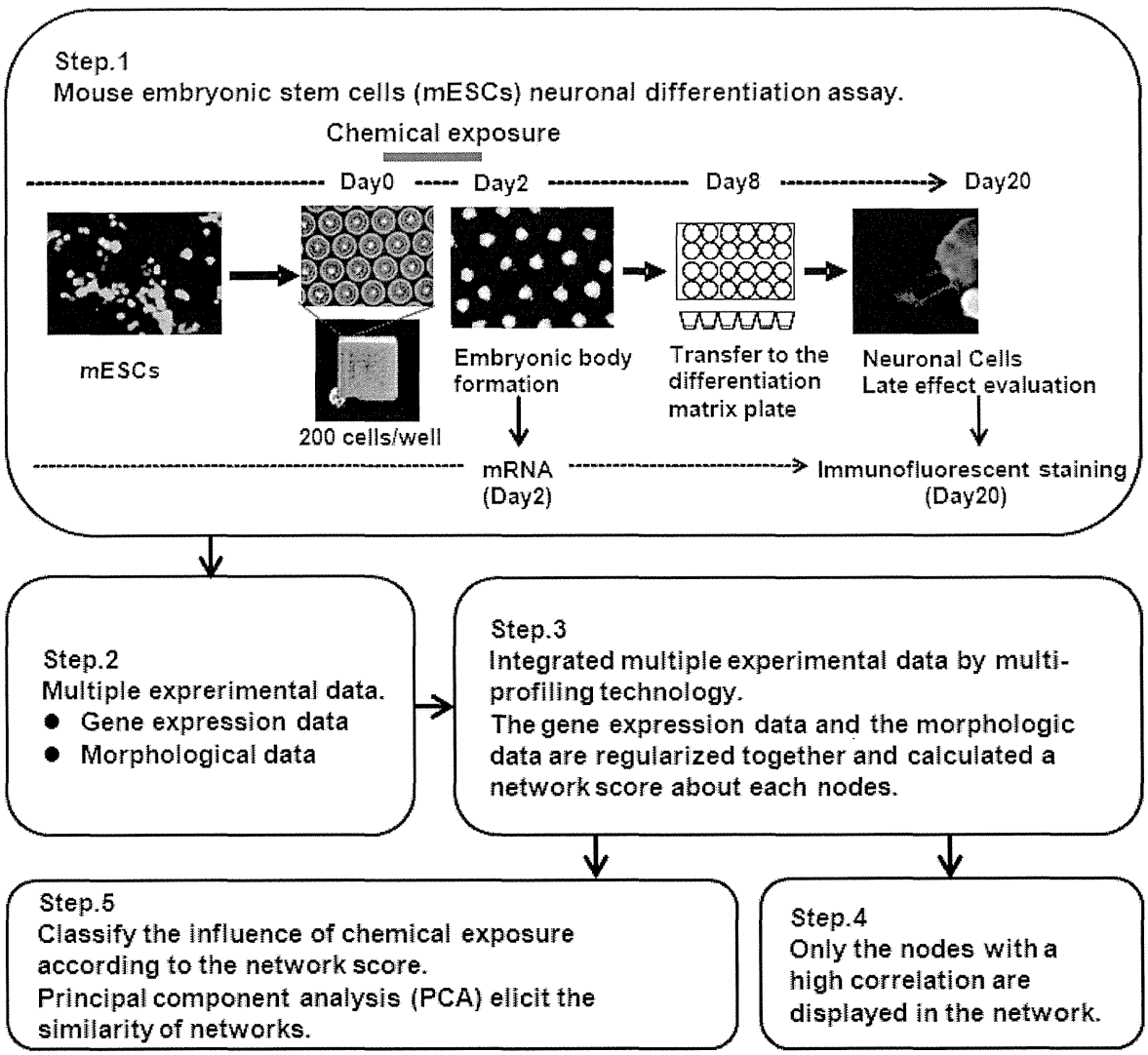

Therefore, the overall aim of this paper is to make a conceptual and methodological proposal to establish a more efficient approach for DNT (Figure 1). More specifically, two objectives are addressed. The first is to describe the DNT design and to identify multi-parametric profiling networks (MPNs) multiple-index networks for 12 environmental chemicals as examples. These are based on the

gene expression signatures of mESCs and phenotype profiling of neurons differentiated from EBs. The second objective is to suggest an information-predictive approach to detect alterations of fetal programming that can be made operational using BNA. We propose BNA as an operational tool for empirically applying the DNT approach.

2. Results and Discussion

2.1. Phenotype Profiling Based on the Morphology of Differentiated Neuronal Cells by High-Content Image Analysis and Generation of Phenotypic Networks

EBs neurally differentiated into neural cells after transfer to OP/L-coated plates. Effects of the 12 environmental chemicals on neural cell growth and NS morphology are shown in Figure 2. Dexamethazone (Dex), Permethrin (PMT) and 17β-estradiol (E2) significantly increased neurite length, while 4-OH-2′,3,3′,4′,5′-pentachlorobephenyl 107 (PCB), triiodotyronine (T3), Thalidmide (TMD), cyclopamine (CPM) and methoprene acid (MPA) significantly decreased neurite length compared with DMSO control (Figure 2A). In glial fibrillary acidic protein (GFAP) positive glial cells, Dex, 5α-dihydrotestosterone (DHT), bisphenol A (BPA) and PCB significantly increased neurite length, while TMD significantly decreased neurite length (Figure 2B). Chemicals were then classified based on morphological features by MPN analysis to extract and predict their toxicities. 12 phenotypic networks (PNs) were generated from the MPN analysis based on the phenotypes of neuronal cells and NSs. We manually classified three categories out of the12 PNs depending on network structures (Figure 3).

Figure 2. Morphological data of MAP2-positive neurons and glial cells. (**A**) Total length of MAP2-positive neurons per well; (**B**) Total length of glial processes per well. * $P < 0.05$, ** $P < 0.001$ *vs.* the vehicle control (DMSO).

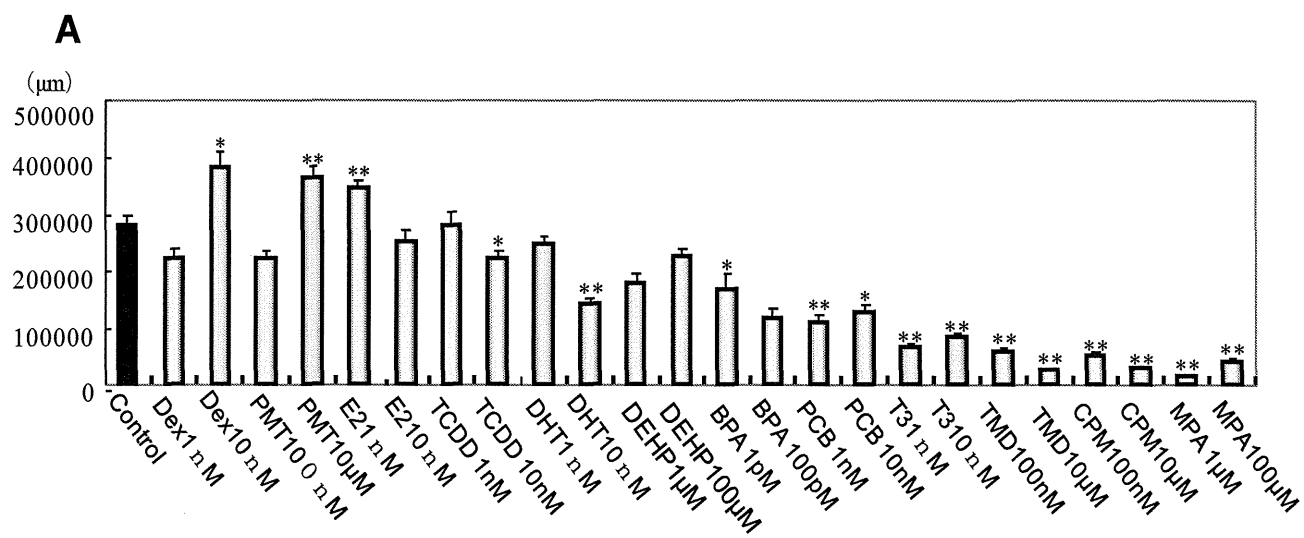

Figure 2. *Cont.*

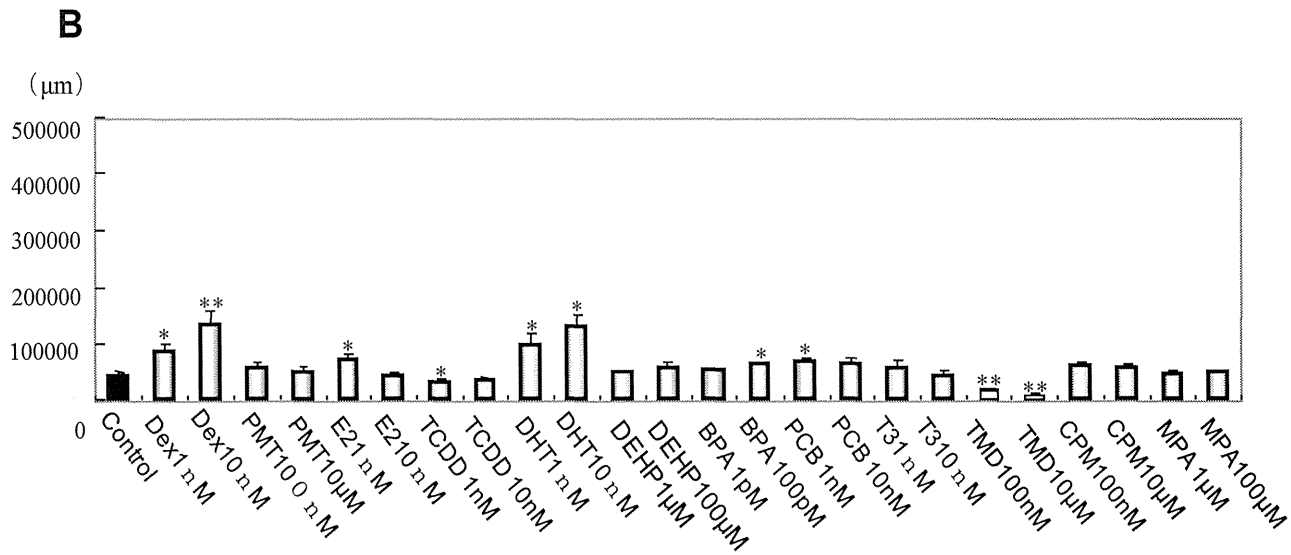

Figure 3. Classification based on morphological imaging and phenotypic feature networks. Class 1: Extension from the turning point is short while the neurite is long; Class 2: Neurite is long and the branch point is complex; Class 3: Neurite is short and there are many nucleus count.

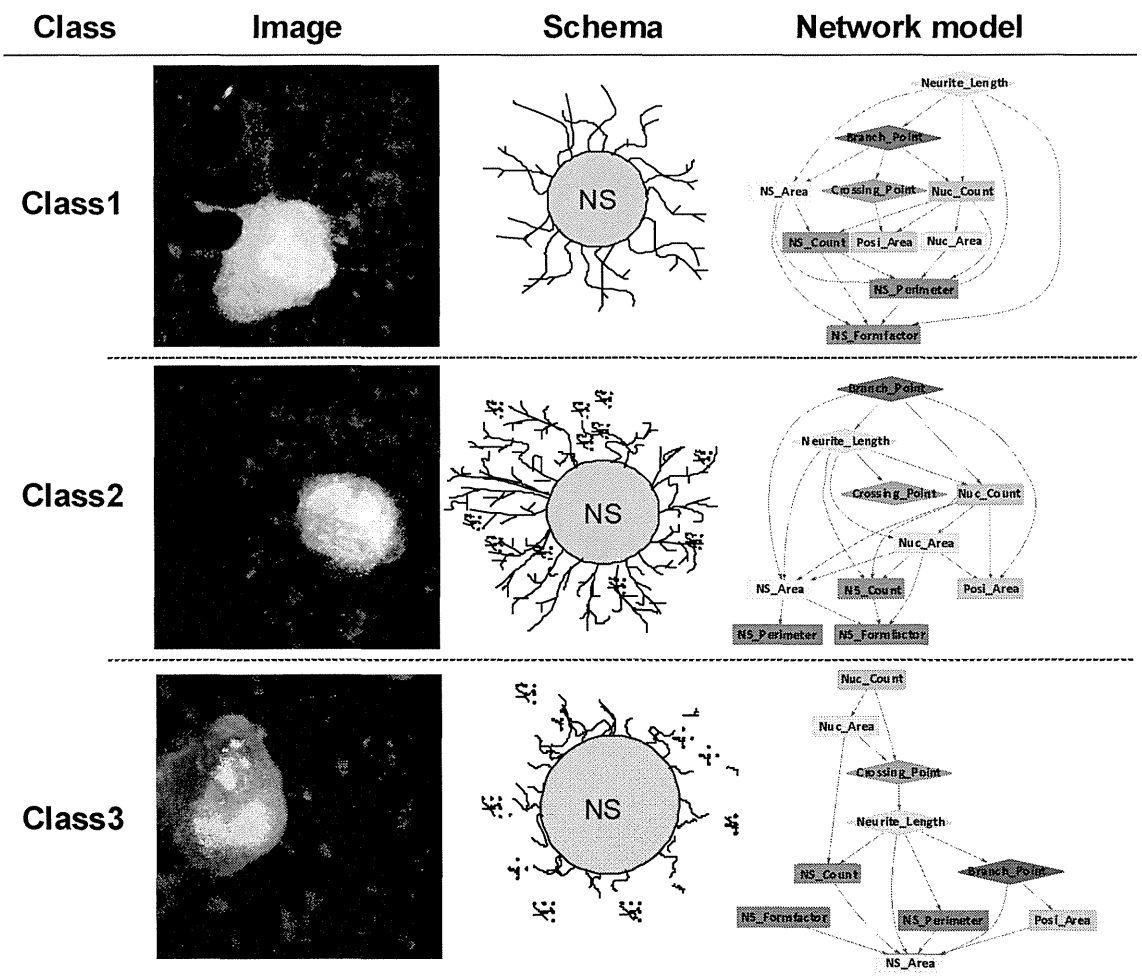

2.2. Generation of a Comprehensive Network Based on Gene Expression and Phenotype Profiling by a Bayesian Network Model

A significant advantage of our unique MPN analysis is that it can predict the correlation coefficient for each pair of nodes, regardless of the data types. Our initial efforts were to derive the interactions between variations of gene expression data after chemical exposure at the early stage of mESC differentiation and effects on the neuronal phenotype data sampled at a later stage of neuronal cell differentiation after EB formation. That is to perform a comprehensive analysis combining data from two different properties. We extracted a discriminative gene group as a gene expression signature from exhaustive genetic profiling, each group was defined by their characteristic category (Table 2) and these gene sets were used in a gene and phenotype interaction network (GPIN) with cell morphological data (Figure 4). To verify whether the MPN analysis can draw out the developmental neurotoxicity, typical examples of DPINs for autism and Parkinson's disease related gene sets exposed to TMD and PMT, respectively, were discussed.

Table 2. Lists of 7 gene sets selected for network analysis.

Alzheimer	Autism	Parkinson	Axon Guidance	Pluripotent	Neural Development	Oxidative-Stress
AR	AR	AR	1500003O03Rik	Arid3b	Atbf1	Aass
ApoE	Cntnap2	Casp3	Abl1	Esrrb	Cdyl	Als2
App	En2	Casp7	Ablim1	Fkbp3	Fos	Apoe
Bace	Esr1	Casp9	Cfl1	Hdac2	Gbx2	Ctsb
Casp3	Esr2	Esr1	Cxcl12	Klf4	Gfap	Dnm2
Casp7	Fmr1	Esr2	Efna4	Mybbp1a	Hras1	Fancc
Esr1	Foxp2	Park2	Epha2	Nacc1	Map2	Gpx7
Esr2	Gabrb3	Park7	Ephb1	Nanog	Mapk1	Gpx8
Ide	Mecp2	RARa	Nfatc2	Nfkbib	Mapk3	Gusb
Il1r1	Nlgn3	RARb	Nfatc3	Nr0b1	Nestin	Hprt1
Mme	RARa	RARg	Ntng1	Nr5a2	Pla2g6	Kif9
Psen	RARb	Slc6a3	Sema3a	Pou5f1	Raf1	Noxo1
RARa	RARg	Snca	Sema3b	Rex1	Rhog	Nxn
RARb	Reln	Th	Sema3d	Sall4	Rif1	Park7
RARg	Slc6a4	Uchl1	Sema3f	Smarcad1	Rps6ka1	Ppp1r15b
Tnfrsf1a	Tsc1		Sema3g	Smarcc1	Sall1	Prdx2
	Tsc2		Sema6a	Sox2	Shc1	Prdx6-rs1
	Ube3a		Sema6b	Sp1	Smarcad1	Psmb5
			Sema6d	Spag1	Sox2	Recql4
			Srgap3	Trim28	Tuj1	Scd1
			Unc5d	Zfp281	Map2k1	Slc41a3
				c-Myc		Sod1
						Sod3
						Txnip
						Txnrd1
						Xpa

Figure 4. Typical example of GPINs for autism and Parkinson's disease gene sets. Gene expression and morphological parameters were connected by the strength of the correlation. GPINs of autism related genes and morphological parameters: (**A**) the vehicle control (DMSO) and (**B**) TMD exposure. GPINs of Parkinson's disease related genes and morphological parameters; (**C**) the vehicle control (DMSO) and (**D**) PMT exposure.

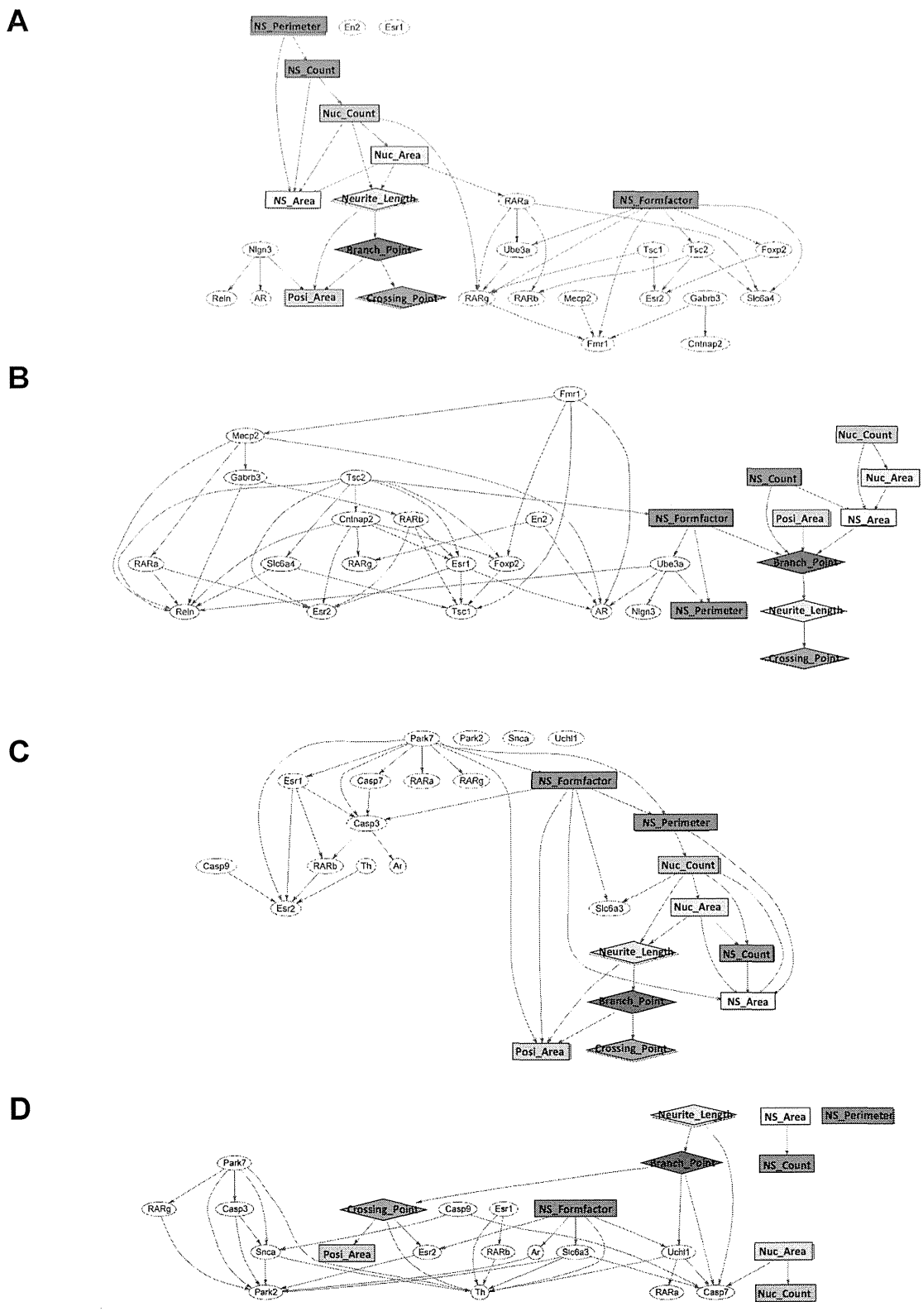

In DMSO control GPIN, RARα positively regulates Fmr1 expression via positive regulation of RARγ expression, suggesting that RA induced neural differentiation could maintain Fmr1 expression. On the other hand, Mecp2, the responsible gene of Rett syndrome, negatively related with Fmr1 expression. It is reasonable because Mecp2 plays a role in the transcriptional repression of methylated genes including Fmr1 [20]. However, in TMD-exposed GPIN, Fmr1 was not regulated by RARs, indicating the neural induction by RA was counteracted by TMD. TMD repressed expression of Fmr1 and Mecp2 and MPN analysis also revealed that Fmr1 positively related with Mecp2 in TMD treated EB derivatives. The results mean that TMD repressed expression of Mecp2 via repression of Fmr1 expression. It seemed to contradict the epigenetic silencing of Fmr1 gene by Mecp2. However, Zhang *et al.* reported that Mecp2 mRNA expression level was drastically decreased in the brains of Fmr1 knockout mice, an animal model of fragile X syndrome of autism spectrum [21]. This means the relationship between Fmr1 and Mecp2 is different between normal and pathological neurons. Additionally, Gabrb3, a subunit of GABA A receptor, was positively affected by Mecp2. In Mecp2 deficient mice, subtle dysfunction of GABAergic neurons contributes to numerous neuropsychiatric phenotypes [22]. The relationship of morphological parameters and gene expression parameters was also changed by TMD. RARs became a hub connecting the genes and morphological parameters and NS_formfactor related to expression of some genes independently from other morphological parameters in DMSO control GPIN. This result suggests that RA induced neural differentiation via RARs, thereby, inducing morphological changes. In TMD-exposed GPIN, the morphological parameters were independent from RARs and the expression of Tsc2 related to them via positive connection with NS_formfactor. These results also indicated a counteraction by TMD against the neural induction by RA. Tcs2 is well known to affect cell proliferation and to control cell size and neural development [23]. Therefore, Tsc2 had a high correlativity to morphological parameters.

Parkinson's disease is the result of degeneration of dopaminergic neuron expressing Th. Recently, some research showed that exposure to pyrethroids including PMT could change the dopaminergic system [24,25]. The genes including in the Parkinson set can be divided into three groups, the ubiquitin pathway (Park2, Snca and Uchl1) and the mitochondrial pathway (Park7, Casp3, Casp7 and Casp9) [26] and genes needed for normal dopaminergic activity (Slc6a3 and Th). In DMSO control GPIN, the ubiquitin pathway genes were not connected into the network. The mitochondrial pathway genes were connected positively but no connection was detected affecting the expression of Th. These results mean that the differentiation of Th positive neuron was not affected by both pathways in normal neuronal differentiation. However, in PMT-exposed GPIN, all genes were connected into the network. Th expression was positively related by Park7, RARβ, Slc6a3 and Uchl1 and negatively related by Snca, Esr1, Crossing_point and NS_formfactor. These results suggest the differentiation of Th positive neuron was affected in a complex manner in PMT exposed EB derivatives. Interestingly, Park7, Casp3, Snca, Park2 and Casp9 were connected indicating the ubiquitin pathway and the mitochondrial pathway affected each other as well as they do in dopaminergic neurons of Parkinson's disease. Th positive neuron might die by apoptosis because we detected the increased expression of Casp3 and Casp9 in addition to these results. Although all morphological parameters were connected to GPIN in DMSO control, the NS morphological parameters (NS_area, NS_count and NS _perimeter) were not connected